Published in final edited form as:
Toxicol Appl Pharmacol. 2011 November 1; 256(3): 249–257. doi:10.1016/j.taap.2011.02.003.

Regulation of Brain Copper Homeostasis by the Brain Barrier Systems: Effects of Fe-Overload and Fe-Deficiency

Andrew D. Monnot, **Mamta Behl**, **Sanna Ho**, and **Wei Zheng***
School of Health Sciences, Purdue University, West Lafayette, Indiana, USA

Abstract

Maintaining brain Cu homeostasis is vital for normal brain function. The role of systemic Fe deficiency (FeD) or overload (FeO) due to metabolic diseases or environmental insults in Cu homeostasis in the cerebrospinal fluid (CSF) and brain tissues remains unknown. This study was designed to investigate how blood-brain barrier (BBB) and blood-SCF barrier (BCB) regulated Cu transport and how FeO or FeD altered brain Cu homeostasis. Rats received an Fe-enriched or Fe-depleted diet for four weeks. FeD and FeO treatment resulted in a significant increase (+55%) and decrease (-56%) in CSF Cu levels ($p<0.05$), respectively; however, neither treatment had any effect on CSF Fe levels. The FeD, but not FeO, led to significant increases in Cu levels in brain parenchyma and the choroid plexus. In situ brain perfusion studies demonstrated that the rate of Cu transport into the brain parenchyma was significantly faster in FeD rats (+92%) and significantly slower (-53%) in FeO rats than in controls. In vitro two chamber Transwell transepithelial transport studies using primary choroidal epithelial cells revealed a predominant efflux of Cu from the CSF to blood compartment by the BCB. Further ventriculo-cisternal perfusion studies showed that Cu clearance by the choroid plexus in FeD animals was significantly greater than control ($p<0.05$). Taken together, our results demonstrate that both the BBB and BCB contribute to maintain a stable Cu homeostasis in the brain and CSF. Cu appears to enter the brain primarily via the BBB and is subsequently removed from the CSF by the BCB. FeD has a more profound effect on brain Cu levels than FeO. FeD increases Cu transport at the brain barriers and prompts Cu overload in the CNS. The BCB plays a key role in removing the excess Cu from the CSF.

Keywords

copper; iron; choroid plexus; blood-CSF barrier; blood brain barrier; in vitro Transwell model; in situ perfusion; ventriculo-cisternal perfusion

Introduction

Copper (Cu) and iron (Fe) are both essential minerals for normal brain function. They play important roles as catalysts, gene expression regulators and second messengers. Both metals are highly reactive and can readily interact with oxygen to form toxic free radicals. The high

* To whom all correspondents should be addressed: Wei Zheng, Ph.D., Professor of Health Sciences, School of Health Sciences, Purdue University, 550 Stadium Mall Drive, CIVL1169, West Lafayette, IN 47907, U.S.A., +1.765.496.6447 (voice), +1.765.496.1377 (fax), wzheng@purdue.edu.

reactivity of both metals, in part, explains why they are in such a high demand for many enzymatic processes and why they are strictly regulated in the body. These two metals are often conjugated with proteins in the serum and cellular compartments, such as transferrin and ferritin for Fe, and ceruloplasmin, albumin and metallothionein for Cu, to prevent the formation of reactive oxygen species (ROS) that cause the damage in the body.

The chemical homeostasis of the central nervous system (CNS) is maintained through the coordinated action of two major brain barrier systems, i.e., the blood-brain barrier (BBB) and the blood-CSF barrier (BCB). The BBB separates the blood circulation from the brain interstitial fluid, and the BCB separates the blood from the cerebrospinal fluid (CSF). Both barriers selectively transport essential nutrients, metals, and drug molecules into the CNS. During the past decades, there has been a substantial research effort on the understanding of the role of brain barriers in metal transport and toxicity (Zheng et al. 1991; 1996; 2001a; 2001b; 2003). Notable work by this group includes lead (Pb), iron (Fe), copper (Cu) and manganese (Mn) (Choi and Zheng, 2009; Shi and Zheng, 2007; Wang et al., 2006; 2008). While Fe transport across the brain barriers has received considerable attention over the years, Cu transport across these barriers has only started to receive attention recently.

Available experimental evidence suggests an intimate relationship between the metabolic roles of Cu and Fe in humans (Fairweather-Tait et al., 2004; Gambling et al., 2004,Sharp et al., 2004). Recent research has shown that intestinal Cu transport is enhanced in rats during Fe deficiency (FeD), indicating that Cu may play a role in various aspects of overall body Fe homeostasis (Collins et al., 2006). With FeD being one of the most common nutritional disorders in the world affecting up to two billion people worldwide (World Health Organization, 2007), there are clearly public health issues associated with imbalances in the nutritional supply of Fe and potentially Cu. In addition, both an excess and deficiency in Cu status is known to be detrimental to the CNS. For example, a mutation in the Cu exporter ATP7A in Menke's disease results in severe Cu deficiency in the brain. Affected individuals display psychomotor deterioration, extensive neurodegeneration in brain grey matter, and an ultimate failure to survive. In Wilson's disease, the mutated ATP7B, another form of Cu exporter in the liver, fails to eliminate excess Cu, leading to the overload of Cu in the brain (Stuerenburg et al., 2000).

A stable metal ion homeostasis is essential for brain's normal function as many metals are required as cofactors for a variety of enzymes. Abnormal Cu homeostasis both systemically and subcellularly, is believed to be associated with the pathogenesis of Parkinson's disease (Gagelli et al., 2006). Evidence has also suggested that FeD may play a critical role in the poor cognitive functioning and the pathogenesis of Alzheimer's disease (Sparks et al., 2003; Murray-Kolb and Beard, 2007; Carlson et al., 2008; Youdim et al., 2008). Carlson et al. (2008) report that FeD alters the expression of genes implicated in Alzheimer's disease. Most recently a study by Salustri et al. (2010) demonstrates that the cognitive function is inversely correlated with serum free Cu levels; as Cu levels rise, the cognitive function declines. While Fe and Cu interactions are known from the literature, the questions as to whether FeD altered Cu homeostasis in the brain and CSF and how exactly FeD affected Cu transport at the BBB and BCB were virtually unexplored.

Previous work from this laboratory suggests that Cu transport into the brain primarily occurs via the BBB as a free Cu ion and that the BCB may serve as a regulatory site for Cu in the CSF (Choi and Zheng, 2009). Cu may enter the brain through various Cu transporters located at the brain barriers such as Cu transporter-1 (Ctr1), divalent metal transporter-1 (DMT-1), ATP7A, and ATP7B (Choi and Zheng, 2009). However, the mechanism by which Cu is sequestered and transported by the brain barriers and the impact of Fe status on these processes remained largely unknown.

The purpose of this study was to (1) establish a relationship between Fe and Cu in the CNS following FeD or Fe overload (FeO); (2) determine whether such a relationship between brain Fe and Cu was maintained by Fe effect on Cu transport at the brain barriers; and (3) understand the direction of free Cu transport between the blood and CSF across the BCB under normal conditions. The study would enable us to understand the role of the brain barriers in regulating Cu homeostasis and the impact of FeO and FeD on CNS Fe and Cu homeostasis.

Materials and Methods

Materials and animals

Chemicals and reagents were obtained from the following sources: copper chloride, sodium pyruvate, calcium chloride and HEPES from Sigma Chemical Company; Hank's balanced salt solution (HBSS), fetal bovine serum (FBS), Dulbecco's modified Eagle's medium (DMEM), and antibiotic-antimycin solution from Gibco (Grand Island, NY); epidermal growth factor (EGF) from Roche Applied Science (Indianapolis, IN); pronase and protease from Calbiochem (La Jolla, CA); and collagen-coated Transwell-COL inserts from Corning (Cambridge, MA). The appropriate rat chow was purchased from Dyets Inc. (Bethlehem, PA). All reagents were analytical grade, HPLC grade, or the best available pharmaceutical grade.

^{14}C-sucrose (specific activity: 495 mCi/mmol) was purchased from Moravek Biochemicals, Inc. (Brea, CA) and Eco-lite-(+) scintillation cocktail from MP Biomedicals (Irvine, CA). $^{64}CuCl_2$ (specific activity 15–30 mCi/μg) was obtained from Washington University at St. Louis, which was produced by cyclotron irradiation of an enriched ^{64}Ni target by using methods reported (McCarthy et al., 1997).

Male Sprague Dawley rats were purchased from Harlan Sprague-Dawley Inc. (Indianapolis, IN). At the time of use the rats were 5 weeks old weighing 125-149 g. They were housed in a temperature-controlled room under a 12-h light/12-h dark cycle. The protocol using rats in this report was approved by Purdue Animal Care and Use Committee.

Experimental Design

Study 1 (n=6 for each group) was performed to establish the normal physiological values of Cu and selected essential metals in the serum, CSF, brain parenchyma, and choroid plexus in order to investigate how FeO or FeD may affect these values. Rats were randomly divided into 3 groups: a control group that was fed with a normal diet (35 mg Fe/kg), an FeD group which received an FeD diet (3-5 mg Fe/kg), and an FeO group whose diet contained an excess amount of Fe (20 g carbonyl Fe/kg) (Dyets Inc.). Animals in each group took the respective diets and distilled-deionized water at libertum for 4 weeks; the dose paradigm was adapted from reports by Dallman et al. (1982) and Ryu et al. (2004). The body weight of the animals was recorded twice a week. After 4 weeks, animals were sacrificed and the appropriate tissues were collected for ICP-MS analysis.

Study 2 (n=5 for each group) was performed to determine the effect of Fe status on the unidirectional uptake rate of Cu (K_{in}) in brain capillaries, brain parenchyma, CP, and CSF. Free unbound ^{64}Cu (5μM) was perfused in situ to brains.

Study 3 (n=4 for each group) was performed to determine the directional transport of Cu across the blood-CSF barrier under normal conditions. A primary choroidal epithelial cell culture model in a two-chamber Transwell system as previously established in the laboratory (Zheng et al., 1998) was used.

Study 4 (n=5-6 for each group) was performed to determine the effect of Fe status on the clearance of Cu by the CP from the CSF. A ventriculo-cisternal perfusion technique established in this laboratory (Wang et al. 2008) was used.

Assessment of serum Fe status and metals in tissues

Serum Fe status was analyzed by quantifying total serum Fe, unsaturated Fe binding capacity (UIBC), total Fe binding capacity (TIBC), and transferrin saturation (TS, %) in serum. Total Fe and UIBC were determined using an Iron/TIBC testing kit (Pointe Scientific, Inc.). The TIBC was calculated as the sum of total serum Fe and UIBC. The TS were determined by dividing total serum Fe by TIBC.

For ICP-MS metal analysis, samples were transferred to a Teflon 96-well plate and digested with 0.15 mL of concentrated HNO_3 (Mallinckrodt, AR Select grade) at 110°C for 4 h. Each sample was diluted to 1.45 mL with 18-MΩ water and analyzed on a PerkinElmer Elan DRCe ICP-MS. Indium (EM Science) was used as an internal standard.

In situ brain perfusion study

A brain perfusion technique has been well established and used in this laboratory (Choi and Zheng, 2009; Deane et al., 2004). Rats from the control, FeD or FeO group were anesthetized with an intraperitoneal (i.p.) injection of ketamine/xylazine (75:10 mg/mL, 1 mL/kg), the neck shaved, and the animal placed on a warming pad. Following the ligation of the external carotid and common carotid arteries, the right internal carotid artery was cannulated with a polyethylene catheter tubing (PE-10) containing a 95% O_2 – 5% CO_2 saturated and continuously gassed 37°C Ringer's solution (in 1000 mL: NaCl 7.31 g, KCl 0.356, $NaHCO_3$ 2.1 g, KH_2PO_4 0.166 g, $MgSO_4$-$7H_20$ 0.3 g, glucose 1.5 g, sodium pyruvate 0.11 g, and $CaCl_2$ 0.278 g, pH 7.4) at a flow rate of 2.9 mL/min (Heidolph Pumpdrive 5201). The “hot” solution was kept in a separate syringe and contained ^{14}C-sucrose (as a space marker) and 5 μM ^{64}Cu in pre-gassed Ringer's solution, was perfused in the cannulated internal carotid artery via a second syringe pump (Harvard Compact Infusion Pump, Model 11 Plus) at a flow rate of 1 mL/min. The total flow rate of the perfusion was therefore 3.9 mL/min. To prevent recirculation of the rat blood, the left ventricle of the heart was cut at the start of the perfusion. This technique has been validated for CNS transport studies (Takasato et al., 1984; Smith, 1996; Zlokovic et al., 1986; Deane and Bradbury, 1990), and is well established in this laboratory (Deane et al., 2004; Choi and Zheng, 2009).

At the end of the perfusion (5 min), the Harvard syringe pump was switched off and the brain vascular system was washed for 1 min with the Ringer solution to remove Cu adsorbed to the luminal surface and the luminal content. Immediately after perfusion, a sample of CSF was collected from the cisterna magna, using a 25-guate butterfly needle (Becton Dickinson, Franklin Lakes, NJ). The brain was harvested and washed with ice-cold saline. The ipsilateral CP tissue was collected from the lateral brain ventricles and the ipsilaterally perfused cerebrum was used for capillary extraction.

Capillary separation

The brain capillary separation was carried out as previously described (Preston et al., 1995; Triguero et al., 1990; Zlokovic, 1995; Deane et al., 2004; Choi and Zheng, 2009). Briefly, the brain was weighed and homogenized in 3 volumes of ice-cold buffer, with 7 strokes in a 7-mL grind pestle (Kontes, Vineland, NJ). The buffer contained (mmol/L) HEPES, 10; NaCl, 141; KCl, 4; $MgSO_4$, 1; NaH_2PO_4, 1; $CaCl_2$, 2.5; and glucose, 10 at pH 7.4. Dextran 70 was added to a final concentration of 15% (w/v) and the solution homogenized with 3 additional strokes. The homogenate was then spun at 5,400 ×g for 15 min at 4°C. The supernatant (brain parenchyma) and pellet (capillary-enriched fraction) were separated

carefully, and counted for radioactivity (in-situ perfusion) or analyzed for metal content via ICP-MS.

Calculation of uptake kinetics

^{64}Cu uptake was expressed as a volume of distribution, V_d, and calculated as (C_{Tissue}/$C_{Perfusate}$ or C_{CSF}/$C_{Perfusate}$), where C_{Tissue} or C_{CSF} are d.p.m./g of brain tissue (e.g. cerebral capillaries, choroid plexus, brain parenchyma, etc.) or CSF, and $C_{Perfusate}$ are d.p.m./mL of the perfusion fluid. The unidirectional uptake rates, K_{in} (μL/s/g), corresponding to the slope of the uptake curve was determined using linear regression analysis of V_d against the perfusion time (T, s) as $V_d=K_{in}$ $T+V_i$, where $V =_i$ is the ordinate intercept of the regression line. ^{64}Cu uptake was corrected for residual radioactivity by deducting V_d for ^{14}C-sucrose from the total ^{64}Cu distributing volume (Choi and Zheng, 2009).

Two-chamber Transwell transport system with primary choroidal cells

The method to culture primary choroidal cells has been well established in this laboratory (Zheng et al., 1998). CP tissues from 4-week old rats were dissected and digested in Hank's balanced salt solution (HBSS) containing 0.2% pronase at 37°C for 10-15 minutes. The digested cells were then washed twice with HBSS and resuspended in growth DMEM medium containing 10% FBS, 100 units/mL penicillin, 100 μg/mL streptomycin, 0.25 μg/mL amphotericin, 100 μg/mL gentamycin and 10 ng/mL epidermal growth factor (EGF). A 20-gauge needle was used to pass cells through 14-15 times to ensure adequate cell separation for seeding. Cells stained with 0.4% Trypan blue were counted under a light microscope before seeded on 35-mm Petri dishes (pre-coated with 0.01% collagen) at a density of 2-3 × 10^5 cells/mL. The cultured cells were maintained at 37°C with 95% air-5% CO_2 in a humidified incubator without disturbance for at least 48 hrs. The growth medium was replaced 3 days after the initial seeding and every 2 days thereafter.

After cultured in dishes for 7-10 days, the cells were transferred to a Transwell transport device which is composed of two chambers. The inner chamber, also known as the apical chamber, is immersed in the outer chamber. When ^{64}Cu was added to the inner chamber and the radioactivity measured in the outer chamber (i.e. transport from the inner to the outer chamber) the experiment was referred to as an efflux study. Likewise, the same experiment done from the outer chamber to the inner chamber was referred to as an influx study. Overnight medium incubation in the Transwell was to improve the cell attachment to the collagen coated membrane in the inner chamber. In the following day, an aliquot of 0.8-mL cell suspension (23 × 10^5/mL for initial seeding) was added to the inner chamber and 1.2 mL of medium was added to the outer chamber. The transepithelial electrical resistance (TEER), an indicator of the tightness of the barrier, was used to track the formation of a cellular monolayer between the inner and outer chambers. The TEER value was measured every other day by an Epithelial Volt-Ohmmeter (EVOM, World Precision Instruments, Sarasota, FL) until the resistance was 50-60 Ω-cm^2. The same two-chamber system without cells was used as the blank and its background was subtracted from the measured TEER. When the cells grew to a confluence, the surface level of the medium in the inner chamber was roughly 2 mm above that of the outer chamber. This in vitro system mimicking the blood-CSF barrier has been used in our previous studies (Zheng et al., 1998; Crossgrove et al., 2004; Shi et al., 2005; Wang et al., 2008; Behl et al., 2009).

In Vitro transepithelial Cu transport study

To investigate the directional transepithelial transport of Cu across the BCB, an aliquot of $^{64}CuCl_2$ was mixed with 150 μL of ^{14}C-sucrose (specific activity: 495 mCi/mmol) to a final concentration of 5 μM $CuCl_2$ (specific activity 5 μCi/mL) and 1 μM with 0.5 μCi/mL ^{14}C-sucrose in HBSS. All the transport parameters were conducted in an incubator kept

at 37°C. For the influx study, ^{64}Cu-containing HBSS was added to the outer chamber (donor) and an aliquot of medium was taken as the initial donor radioactivity. A series of time points (0, 5, 10, 15, 30, 45, 60, 75, 90 min, 2, 3, 4 h) were set for sample collection. At each time point, an aliquot of 10 μL of HBSS was taken from the inner (receiver) chamber and replaced with an equal volume of fresh HBSS. The efflux study was conducted in the exact same manner except the inner chamber was the donor chamber and the outer chamber was the receiver.

All samples were counted by an auto-Gamma 5000 Series Gamma Counter (Packard Instrument Company). To count ^{14}C-sucrose the samples were mixed with Eco-lite cocktail and counted on a Packard Tr-Carb 2900 TR Liquid Scintillation Analyzer.

Calculations of transepithelial transport parameters

To determine the transport coefficient for ^{64}Cu and ^{14}C-sucrose across the cellular monolayer, the data within the linear range were used for linear regression analyses. The slope (d.p.m./mL-min) of each dataset was used to calculate the total and blank permeability coefficients in Eq. (1),

$$P_T \text{ or } P_B = \frac{V_R}{A} \Delta C_R / (C_D \Delta t) \quad (1)$$

where P_T represents the total permeability coefficient (cell monolayer + membrane + coating, cm/min); P_B, the blank permeability coefficient (membrane + coating, cm/min); V_R, volume of media in the receiver chamber; A, surface area of transport membrane (1.1 cm^2); C_D, concentration of radiolabeled compounds in donor chamber (d.p.m./mL); C_R, concentration of radiolabeled compounds in receiver chamber (d.p.m./mL). The permeability coefficients of epithelial barrier (P_E) are then obtained from the Eq. (2) (Shi and Zheng, 2005; Wang et al., 2008).

$$\frac{1}{P_E} = \frac{1}{P_T} - \frac{1}{P_B} \quad (2)$$

where P_E is the permeability coefficient of epithelial barrier.

In situ ventriculo-cisternal perfusion

Control, FeD and FeO rats were anesthetized with an i.p. injection of ketamine/xylazine (75:10 mg/mL, 1 mL/kg) and immobilized in a stereotaxic device. A midline cutaneous incision was made from the forehead to the neck, exposing the top of the skull. A hole was drilled for insertion of a guide cannula (Plastics One Inc., Roanoke, VA). The cannula was inserted into the lateral ventricle according to the following parameters on three scales: 0.8 mm posterior to the bregma, 1.4 mm lateral to the midline, and 3.5 mm vertical from the surface of the skull (Wang et al., 2008). An internal guide cannula connected to PE50 tubing was inserted into the guide cannula for lateral ventricle perfusion controlled by the pump-driven syringe filled with artificial CSF (aCSF). Pre-gassed aCSF containing either 0.5 μCi/mL of ^{14}C-sucrose or 2 μM of $CuCl_2$ was delivered to the lateral ventricle at a rate of 28 μL/min controlled by a syringe pump (Harvard Compact Infusion Pump, Model 11 Plus). A 26G butterfly needle was inserted at an appropriate angle into the cisterna magna for collection of the perfusion outflow. Cisternal outflow samples were collected at 10-min intervals throughout the perfusion time (80 min). The CSF volume was determined by

measuring its weight assuming the CSF density was 1 g/mL. Additional anesthesia was given to the rats as needed. Body temperature was maintained at 37°C using a heating pad during the perfusion. At the end of the perfusion, the animal was decapitated, the brain removed, and both lateral choroid plexus tissues were harvested. Samples were taken for liquid scintillation counting and ICP-MS.

Statistics

All data are expressed as mean ± SEM unless stated otherwise. Statistical analyses of the differences between groups were carried out by one-way ANOVA, and the Pearson correlations were determined using SPSS 17.0 statistic package for Windows. Linear regression lines were plotted with Microsoft Excel 2007. The differences between the means were considered significant if P values were equal or less than 0.05.

Results

Fe concentrations and related parameters in FeO or FeD rats

Both FeO and FeD treatment in diet resulted in the hematological changes one would expect to find in the serum of individuals who are overloaded or deficient with Fe, i.e., a nearly 2-fold increase in serum Fe in FeO animals compared to controls ($p<0.05$) and a marked, yet nearly significant decrease in serum Fe in FeD animals ($p=0.072$) (Fig. 1A). A more sensitive ICP-MS analysis revealed that FeD animals had roughly half the amount of Fe as compared to controls ($p<0.05$; Fig. 2A). The change in UIBC was as expected in FeO and FeD animals with FeO having significantly less iron binding capacity and FeD animals having greater Fe binding capacity ($p<0.05$; Fig. 1B). The TIBC was elevated in FeD animals and unchanged in FeO animals ($p<0.05$; Fig. 1C), while transferrin saturation was elevated in FeO animals and decreased in FeD ($p<0.05$; Fig. 1D). These results indicate that the animals were rendered either overloaded of deficient of Fe through the dietary regiment.

Quantitation of Fe levels in the serum, CSF, and brain parenchyma by ICP-MS analysis indicated that FeO treatment significantly elevated Fe concentrations in both the serum and brain parenchyma (Fig. 2A, C). Interestingly, treatment with FeD diet also resulted in a significant increase of Fe level in brain parenchyma (Fig. 2C), although serum Fe was indeed decreased in these animals (Fig. 2A). Neither FeO nor FeD treatment had any effect on Fe levels in the CSF (Fig. 2B).

Cu concentrations in serum, brain parenchyma, choroid plexus and CSF as affected by FeO or FeD

Following FeO treatment, Cu concentrations in serum and CSF were significantly decreased by 97% ($p<0.05$), and 56% ($p<0.02$), respectively (Fig. 3A, B). In contrary, the Cu concentrations were significantly elevated in the brain, CSF and choroid plexus in FeD rats by 85 % ($p<0.05$), 52% ($p<0.05$), and 67% ($p<0.05$), respectively (Fig. 3B, C, D). Noticeably, the magnitude of changes in serum Cu levels was much greater in FeO rats (nearly 40 fold decrease) than in FeD rats. In contrast with CSF Fe levels, where both FeO and FeD had no detectable effect on CSF Fe, the CSF concentration of Cu was significantly lower in FeO rats and significantly higher in FeD rats than those in controls, suggesting a direct impact of systemic Fe homeostasis on Cu regulation by brain barrier systems and thereupon an altered Cu level in the CSF. Interestingly, both FeO and FeD treatments led to an elevated Cu concentration in brain parenchyma (Fig. 3C).

Further linear regression analysis revealed that CSF Cu levels were inversely associated with serum Fe levels ($r=-0.665$, $p<0.01$, Fig. 4A). However, no significant association was found between serum Fe and CSF ($r=0.065$, $p=0.812$, Fig. 4B) or in capillary depleted brain

parenchyma (r=-0.164, p=0.543, Fig. 4C). An inverse association, which approached but did not reach statistical significance, was found between serum Fe and choroid plexus Cu (r=-0.419, p=0.106, Fig. 4D), whereas strong positive correlations were found between Fe and Cu in the choroid plexus (r=0.738, p<0.01, Fig. 5A) as well as in brain parenchyma (r=0.781, p<0.01, Fig. 5B).

Transport of ^{64}Cu by brain barriers as affected by FeO and FeD treatment

The above results prompted us to further explore whether Fe status altered the transport rate of Cu across the brain barriers. Unidirectional rate constants (K_{in}) represent the rate of ^{64}Cu entering a particular compartment after 5 min of perfusion via the intra-carotid artery. In FeO animals, the rate constant for ^{64}Cu transported into brain parenchyma was significantly decreased, about 50% that of controls (Fig. 6A), while the rate constant to brain capillary was not changed in the same group of rats (Fig. 6B). Treatment with FeD greatly increased the transport of ^{64}Cu into brain tissue; the rate constant was increased by nearly 2 fold in FeD animals compared to controls (Fig. 6A). Consistently, the K_{in} of ^{64}Cu into the brain capillaries in FeD animals was nearly 5 times that of controls (Fig. 6B). The rates of Cu transport into the CSF and choroid plexus were also significantly increased (p<0.05) in FeD animals (Fig. 6C, 6D). These finding are consistent with our ICP-MS studies, suggesting an increased influx of Cu into the brain and CSF during FeD.

Two chamber Transwell study of directional transport of Cu by the blood-CSF barrier

When ^{14}C-sucrose, a leakage marker, was added to the donor chamber, the flux of ^{14}C-sucrose in the receiver chamber in either direction, was nearly equal (Fig. 7A), suggesting an equal passive leakage of ^{14}C sucrose molecules across the barrier no matter to which chamber sucrose was added. When ^{64}Cu was added to either the inner or outer chamber to study the direction of Cu transport by the BCB, the primary choroidal epithelia appeared to transport Cu more readily in the direction of efflux (apical to basolateral) than influx, as the permeability rate constant (P_E) for ^{64}Cu was roughly 1.8 fold higher in the efflux study than in the influx study (Fig. 7A). To correct for non-specific leakage across the barrier system, the P_E values of ^{64}Cu were normalized by ^{14}C-sucrose and expressed as a ratio of ^{64}Cu to ^{14}C-sucrose. After correcting for nonspecific leakage, Cu efflux (from the CSF to the blood) in the blood-CSF model was nearly 2 fold greater than that of the influx (p<0.01, Fig. 7B). These results suggested that the efflux of Cu across the blood-CSF barrier was a more favorable pathway for Cu transport than the influx.

Clearance of Cu by the blood-CSF barrier as affected by FeO and FeD treatment

Using an in situ ventriculo-cisternal brain perfusion technique, we investigated Cu clearance from the CSF from control, FeO, and FeD animals. Cu recovered from the cisternal effluent was expressed as the ratio of Cu concentration in the collected effluent to that in the perfusate. As a result of the choroid plexus being the major tissue responsible for removing materials present in the ventricular CSF, a higher recovery of Cu in the cisternal effluent suggests there is less in situ uptake of Cu by this tissue, while less recovery of Cu suggests a greater uptake of Cu by the choroid plexus. In the FeD animals, the Cu recovered in the cisternal effluent was lower than that of both the control and FeO animals (p<0.05), suggesting there was a greater clearance of Cu from the CSF in these animals (Fig. 8A). Since the CSF secretion rate, measured by the use of the space marker ^{14}C-sucrose was not altered by either FeO or FeD (Fig. 8B), the increased Cu clearance from the CSF was apparently due to elevated Cu uptake by the choroid plexus.

ICP-MS analysis of multiple metal concentrations in the serum, CSF, choroid plexus and brain parenchyma

ICP-MS metal analysis revealed numerous changes in metal concentrations as a result of FeO and FeD. Most significantly, we found that the metal concentrations in brain parenchyma and choroid plexus tissues varied as a result of Fe status much more readily than metals in the CSF or serum (Table 1). In the brain parenchyma FeO caused an elevation of Ca^{2+}, Fe^{2+}, Zn^{2+}, Se^{2+}, and Sr^{2+}, while FeD caused increases in Ca^{2+}, Mn^{2+}, Fe^{2+}, Cu^{2+}, Sr^{2+}, and a decrease in Ni^{2+} ($p<0.05$). In the choroid plexus, FeO caused only an elevation of Fe^{2+}, while FeD caused an increase in Ca^{2+}, Fe^{2+}, Co^{2+}, Ni^{2+}, Cu^{2+}, Zn^{2+}, Se^{2+}, and Rb^{2+} ($p<0.05$). It appeared that under the FeD condition, the fluctuation of metal concentrations was more significant in the choroid plexus than in the CSF, perhaps due to the regulatory function of the blood-CSF barrier to actively transport metals between the blood and CSF in order to keep the CSF metal levels constant and to protect the normal brain function.

In serum, FeO caused an increase in Fe^{2+}, and decreases in Cu^{2+}, Rb^{2+}, and Sr^{2+} ($p<0.05$). FeD resulted in decreased Fe^{2+} and elevated Co^{2+}, and Sr^{2+} levels in the CSF ($p<0.05$). There was also an increased serum Cu level although not significant ($p=0.064$). In the CSF, FeO caused decreases in Cu^{2+} and Sr^{2+} levels, and Fe D caused an increase in Cu^{2+} and Se^{2+} levels ($p<0.05$).

Discussion

The results of this study clearly indicate that systemic Fe homeostasis has a significant impact on Cu homeostasis in blood, CSF, choroid plexus and brain parenchymal tissues. More specifically, our results showed the following characteristics of Fe-Cu interactions: (1) Fe levels in the CSF and brain parenchyma appeared to be more tightly regulated than Cu; (2) a decreased serum Fe level in FeD animals seemed likely to increase Cu levels in the choroid plexus and CSF; (3) changes in serum Fe levels affected more profoundly the Cu level in the CSF than in brain parenchyma; and (4) an increase in tissue concentrations of Cu in the choroid plexus and brain parenchyma was associated with the increased Fe level in the corresponding tissues.

A vast amount of evidence in literature has suggested that the homeostasis of Fe and Cu in the body is physiologically intertwined (Crowe et al., 1996; Garrick et al., 2003). Some investigators have suggested that this interaction may take place primarily in intestinal absorption (Arredono et al., 2000;Arredondo and Nunez, 2005; Linder et al., 2003). For example, using an immortalized intestinal epithelial line known as Caco-2 cells, Linder et al. (2003) report that inducing FeD in this in vitro model system causes an increase in both the uptake and retention of Cu. Arredondo et al. (2006) further demonstrate that Cu and Fe display a competitive inhibition with regards to intestinal absorption in Caco-2 cells. These findings are consistent with our own data obtained from the brain barrier systems that systemic FeD apparently caused Cu overload in brain tissues. Also, the serum Fe statuses of these treated animals were similar to those in Ryu et al. 2004, and Dallman et al. 1982, from which our dose paradigm was adopted. In addition, our data clearly demonstrated a strong relationship between Cu and Fe in the serum, CSF, brain parenchyma, and choroid plexus. Considering the overall importance of Cu in disease causation and progression of numerous neurodegenerative disorders, a disrupted Fe homeostasis due to either genetic defects or environmental alteration can perceivably impact significantly the Cu stability of the central nervous system (CNS).

How exactly the changes in Fe homeostasis affect the regulation of Cu in the brain is unknown. Previous studies from this laboratory support the view that both brain barriers

play a major role in regulating brain Cu transport. It is the free Cu, but not protein-bound Cu, that represents the major Cu species being transported across the brain barriers (Choi and Zheng, 2009). The works by Erikson et al. (2004) and Garcia et al. (2007) explore the effect of FeD on divalent metal accumulation in different regions of the brain. FeD resulted in increased brain accumulation of manganese (Mn), zinc (Zn) and Cu in regions such as the globus pallidus, striatum, and substantia nigra (Erikson et al., 2004; Garcia et al., 2007). Our current data are in good agreement with these previous observations with respect to Cu transport by the brain barriers and the impact of Fe status on Cu homeostasis in the CNS. Interestingly, FeO also led to elevated Cu concentration in brain parenchyma in our study. It is well known that the balance of Fe levels are regulated by Cu-dependent extracellular Fe transport protein ceruloplasmin as well as Cu-dependent intracellular Fe transport protein hephaestin. Conceivably, FeO in the brain parenchyma may increase the cellular demand for more of these Cu-dependent Fe transport proteins so as to export the excess Fe to prevent Fe toxicity; this hypothesis, however, needs additional experimental testing. It is possible that this phenomenon is responsible for the positive correlations found between Cu and Fe in both the brain parenchyma and choroid plexus.

In this study we focused on the Cu influx via the BBB to brain parenchyma, as well as its efflux at the BCB by the choroid plexus. In brain parenchyma, the unidirectional uptake (K_{in}) of Cu was roughly 2 fold faster than the uptake rate to the CSF in control animals, indicating that Cu appeared to be transported at a greater rate to the brain parenchyma than to the CSF. Since the parenchyma and CSF are in direct contact with the BBB (parenchyma) and the BCB (CSF), respectively, and since there is no apparent barrier between brain parenchyma and the CSF, it is reasonable to suggest that Cu may enter brain parenchyma from the BBB; subsequently it may flow from the brain parenchyma to the CSF. Interestingly, our in situ studies indicated that the K_{in} for Cu in the choroid plexus, where the BCB locates, was nearly 100 fold faster than the uptake rate in the CSF. Thus, the role of the choroid plexus in regulating Cu in the CSF cannot be ignored.

As a result of the choroid plexus being in contact with both the CSF and blood, it is possible that the high accumulation of Cu in the choroid plexus could come from either the blood, CSF, or both. Subsequently the Cu in the CSF could be derived from either the choroid plexus, or the brain parenchyma. However, it is unlikely that the Cu is being transported from the blood to the choroid plexus and subsequently to the CSF, because the rate of transfer to the CSF was about a 3-4 fold increase in FeD rats, whereas it was only about a 1.5 fold increase in the plexus tissue. Thus, most of the excess Cu in the CSF must come from the interstitial fluid between neurons and glial cells in the brain parenchyma.

To further address the role of choroid plexus in Cu transport, we used a two-chamber Transwell culture system to determine the primary direction through which Cu was transported across the BCB. This in vitro system possesses a number of advantages: (1) it forms a biological barrier that mimics the in vitro BCB (Zheng et al., 1998); (2) the polarized cells on the Transwell membrane can be used to study the orientation of metal transport across the BCB; and (3) the system allows the metal to be added to either side of the barrier system. Using this in vitro BCB model system, we demonstrated that the rate of Cu transport from the CSF to the blood was greater than from the blood to the CSF. Additionally, ventriculo-cisternal perfusion studies provided in vivo evidence to support the role of the choroid plexus in the uptake of Cu from the CSF. Considering the fact that FeD increased Cu uptake at a greater rate in the BBB, brain parenchyma, and CSF, it was tempting to speculate that the BCB may increase the rate of Cu transport from the CSF to blood in an attempt to clear excess CSF Cu. Indeed, FeD animals did display a greater rate of Cu clearance from the CSF compared to either FeO or control animals, while ^{14}C-sucrose clearance, a measure of BCB permeability, was unchanged. Thus both the in vitro and in

vivo data from our current studies support the theory that the BCB's role in CNS Cu homeostasis is to efflux Cu from the CSF to the blood.

Our results demonstrated that FeD appeared to have a more profound effect than FeO on Cu homeostasis at the brain barriers. Our in vivo data showed that FeD increased the rate of Cu transport across the BBB, resulting in elevated Cu levels in all cerebral compartments. In the case of FeO, while the treatment decreased Cu transport in the brain parenchyma, the rates of Cu transport across both the BBB and BCB were unchanged. These seemed to suggest that the brain barriers are better adapted at controlling Cu homeostasis brought on by FeO than FeD. This was also demonstrated by unchanged Cu levels in the brain following FeO. Although FeO caused a significant decrease in serum and CSF Cu levels brain parenchyma Cu levels remained unchanged. It is plausible that the brain barriers and brain interstitial compartment are able to retain adequate Cu stores to perform necessary functions within the CNS. Interestingly, Fe levels in the brain parenchyma and choroid plexus were significantly increased in the FeD animals. This may have occurred as a result of the brain barriers and brain interstitial fluid attempting to maintain a stable Fe homeostasis. It is reasonable to suggest that the brain barriers are able to uptake and retain more Fe in an FeD state to prevent Fe deficiency in the brain. Our ICP-MS data also indicated that the overall metal ion homeostasis was impacted to a much greater extent in both the choroid plexus and brain parenchyma in FeD than in FeO animals (Table 1). While the rationale as to why the brain barrier systems as well as the CNS have a stronger response to FeD than FeO remains to be explored; it is possible the different response of Cu/Fe regulation to FeO and FeD may be the result of sensitivity of metal transporters to the abnormal Fe status.

Several transporters have been suggested to transport Cu across the brain barriers, including Ctr1, DMT1, ATP7A, and ATP7B (Li and Zheng, 2005; Choi and Zheng, 2009). Our recent data suggest a profound expression of DMT1 in the choroid plexus and the FeD-induced upregulation of DMT1 (Data not shown). However, the exact functions of these transporters at the brain barriers in regulating Cu transport and the impact of FeO and FeD on the expression of these transporters are currently still unknown. Studies to investigate Cu transporters localization, regulatory mechanism of their expression, and how the dysregulation of these transporters by FeO and FeD affects brain Cu homeostasis are currently underway in this laboratory.

In summary, the present work indicates that both the BBB and BCB contribute to maintain a stable Cu homeostasis in the brain. The BBB appears to be a more important route than the BCB in the transport of Cu into brain parenchyma; upon entering brain, Cu is utilized and released into the CSF via the interstitial fluid. Subsequently Cu is removed by the BCB from the CSF to blood. FeO increases Fe levels in the brain and serum, and decreases Cu levels in the serum and CSF. In contrast, FeD increases Cu transport at the brain barriers; consequently FeD prompts Cu overload in the CNS. Under the latter condition, the BCB in the choroid plexus plays a key role to remove excess Cu from the CSF so to maintain the Cu homeostasis in the CNS. Further investigation into the mechanism of Cu and Fe transport by the brain barriers under normal and disease states is well warranted.

Acknowledgments

The authors thank Dr. Yanshu (Sue) Zhang's technical assistance. The research reported in this manuscript was supported in part by a Ross Fellowship from the Purdue Research Foundation (ADM) and by NIH/National Institute of Environmental Health Sciences grant RO1-ES008146 and R21-ES017055.

References

Arredondo M, Uauy R, González M. Regulation of copper uptake and transport in intestinal cell monolayers by acute and chronic copper exposure. Biochem Biophys Acta. 2000; 1474(2):169–76. [PubMed: 10742596]

Arredondo M, Munoz P, Mura CV, Nunez MT. DMT-1, a physiologically relevant apical Cu1+transporter in intestinal cells. Am J Physiol Cell Physiol. 2003; 284:C1525–C1530. [PubMed: 12734107]

Arredondo M, Nunez MT. Iron and copper metabolism. Molecular Aspects of Medicine. 2005; 26:313–327. [PubMed: 16112186]

Arredondo M, Martinez R, Nunez MT, Ruz M, Olivares M. Inhibition of iron and copper uptake by iron, copper, and zinc. Bio Res. 2006; 39:95–102. [PubMed: 16629169]

Burdo JR, Menzies SL, Simpson IA, Garrick LM, Garrick MD, Dolan KG, Haile DJ, Beard JL, Connor R. Distribution of divalent metal transporter 1 and metal transport protein 1 in the normal and Belgrade rat. J of Neurosci Res. 2001; 66(6):1198–1207. [PubMed: 11746453]

Carlson ES, Magid R, Petryk P, Georgieff MK. Iron deficiency alters expression of genes implicated in Alzheimer disease pathogenesis. Brain Res. 2008; 1283:75–83. [PubMed: 18723004]

Choi BS, Zheng W. Copper transport to the brain by the blood-brain barrier and blood-CSF barrier. Brain Res. 2009; 1258:14–21. [PubMed: 19014916]

Collins J. Gene chip analyses reveal differential genetic responses to iron deficiency in rat duodenum and jejunum. Biol Res. 2006; 39(1):25–37. [PubMed: 16629162]

Crowe A, Morgan EH. Iron and copper interact during their uptake and deposition in the brain and other organs of developing rats exposed to dietary excess of the two metals. Journal of Nutrition. 1996; 126(1):193–94.

Dallman PR, Refino C, Yland MJ. Sequence of development of iron deficiency in the rat. Am J Clin Nutr. 1982; 35(4):671–677. [PubMed: 6280487]

Deane R, Bradbury MW. Transport of lead-203 at the blood-brain barrier during short cerebrovascular perfusion with saline in the rat. J Neurochem. 1990; 54:905–914. [PubMed: 2106011]

Deane R, Zheng W, Zlokovic BV. Brain capillary endothelium and choroid plexus epithelium regulate transport of transferrin-bound and free iron into the rat brain. J Neurochem. 2004; 88:813–820. [PubMed: 14756801]

Erikson KM, Syversen T, Steinnes E, Aschner M. Globus pallidus: a target brain region for divalent metal accumulation associated with dietary iron deficiency. J Nut Bio. 2004; 15(6):335–341.

Fairweather-Tait SJ. Iron nutrition in the UK: getting the balance right. Proc of the Nutrition Society. 2004; 63:519–528.

Gaggelli E, Kozlowski H, Valensin D, Valensin G. Copper homeostasis and neurodegenerative disorders (Alzheimer's, prion, and Parkinson's diseases and amyotrophic lateral sclerosis). Chem Rev. 2006; 106(6):1995–2044. [PubMed: 16771441]

Gambling L, McArdle HJ. Iron, copper, and fetal development. Proc of the Nutrition Society. 2004; 63:553–562.

Garcia SJ, Gellein K, Syversen T, Aschner M. Iron deficient and manganese supplemented diets alter metals and transporter in the developing rat brain. Toxic Sci. 2007; 95(1):205–214.

Garrick MD, Nunez MT, Olivares M, Harris ED. Parallels and contrasts between iron and copper metabolism. Biometals. 2003; 16:1–8. [PubMed: 12572661]

Kodama H. Essential trace elements and immunity. Niphon Rinsho. 1996; 54:46–51.

Linder MC, Zerounian NR, Moriya M, Malpe R. Iron and copper homeostasis and intestinal absorption using the Caco2 cell model. BioMetals. 2003; 16:145–160. [PubMed: 12572674]

McCarthy DW, Shefer RE, Klinkowstein RE, Bass LA, Margeneau WH, Cutler CS, Anderson CJ, Welch MJ. Efficient production of high specific activity ^{64}Cu using a biomedical cyclotron. Nucl Med Biol. 1997; 24:35–43. [PubMed: 9080473]

Murray-Kolb LE, Beard JL. Iron treatment normalizes cognitive functioning in young women. Am J Clin Nutr. 2007; 85:778–787. [PubMed: 17344500]

Preston JE, al Sarraf H, Segal MB. Permeability of the developing blood-brain barrier to 14C-mannitol using the rat in situ brain perfusion technique. Brain Res Dev Brain Res. 1995; 87:69–76.

Ryu DY, Lee SJ, Park DW, Choi BS, Klaassen CD, Park JD. Dietary iron regulates intestinal cadmium absorption through iron transporters in rats. Toxicology Letters. 2004; 152:19–29. [PubMed: 15294343]

Salustri C, Barbati G, Ghidoni R, Quintiliani L, Ciappina S, Binetti G, Squitti R. Is cognitive function linked to serum free copper levels? A cohort study in a normal population. Clin Neurophysiol. 2010; 121(4):459–60. 2010 Apr. [PubMed: 20071223]

Sharp P. The molecular basis of copper and iron interactions. Proc Nutritional Society. 2004; 63:563–569.

Shi LZ, Zheng W. Establishment of an in vitro brain barrier epithelial transport system for pharmacological and toxicological study. Brain Res. 2005; 1057:37–48. [PubMed: 16126179]

Shi LZ, Zheng W. Early lead exposure increases the leakage of the blood-cerebrospinal fluid barrier, in vitro. Human Exp Toxicol. 2007; 26:159–167.

Smith QR. Brain perfusion systems for studies of drug uptake and metabolism in the central nervous system. Pharm Biotechnol. 1996; 8:285–307. [PubMed: 8791815]

Sparks DL, Schreurs BG. Trace amounts of copper in water induce β-amyloid plaques and learning deficits in a rabbit model of Alzheimer's disease. Proc Natl Acad Sci USA. 2003; 100(19):11065–11069. [PubMed: 12920183]

Stuerenburg HJ. CSF copper concentrations, blood-brain barrier function, and ceruloplasmin synthesis during the treatment of Wilson's disease. J Neural Transm. 2000; 107:321–329. [PubMed: 10821440]

Takasato Y, Smith QR. An in situ brain perfusion technique to study cerebrovascular transport in the rat. Am J Physiol. 1984; 247:H484–H493. [PubMed: 6476141]

Triguero D, Buciak J, Pardridge WM. Capillary depletion method for quantification of blood-brain barrier transport of circulating peptides and plasma proteins. J Neurochem. 1990; 54:1882–1888. [PubMed: 2338547]

Wang X, Li GJ, Zheng W. Up regulation of DMT1 expression in choroidal epithelia of the blood-CSF barrier following manganese exposure in vivo. Brain Res. 2006; 1097:1–10. [PubMed: 16729984]

Wang X, Li GJ, Zheng W. Efflux of iron from the cerebrospinal fluid to the blood at the blood-CSF barrier: effect of manganese exposure. Exp Biol Med. 2008; 233(12):1561–1571.

World Health Organization. Micronutrient deficiencies. 2007. Retrieved from http://www.who.int/nutrition/topics/ida/en/index.html

Youdim MBH. Brain iron deficiency and excess; cognitive impairment and neurodegeneration with involvement of striatum and hippocampus. Neurotoxicity Res. 2008; 14(1):45–56.

Zheng W, Perry DF, Nelson DL, Aposhian HV. Protection of cerebrospinal fluid against toxic metals by the choroid plexus. FASEB J. 1991; 5:2188–2193. [PubMed: 1850706]

Zheng, W. The choroid plexus and metal toxicities. In: Chang, LW., editor. Toxicology od metals. CRC Press; New York: 1996. p. 609-626.

Zheng W, Zhao Q, Graziano JH. Primary culture of choroidal epithelial cells: characterization of an in vitro model of blood-CSF barrier. In vitro Cell Dev Animal. 1998; 34:40–45.

Zheng W. Toxicology of choroid plexus: special reference to metal-induced neurotoxicities. Microsc Res Techn. 2001a; 52:89–103.

Zheng W. Neurotoxicology of the brain barrier system: new implications. J Toxicol Clin Toxicol. 2001b; 39:711–719. [PubMed: 11778669]

Zheng W, Aschner M, Ghersi-Egea JF. Brain barrier systems: a new frontier in metal neurotoxicological research. Toxicol Appl Pharmacol. 2003; 192:1–11. [PubMed: 14554098]

Zlokovic BV, Begley DJ, Djuricic BM, Mitrovic DM. Measurement of solute transport across the blood-brain barrier in the perfused guinea pig brain: method and application to N-methyl-alpha-aminoisobutyric acid. J Neurochem. 1986; 46:1444–1451. [PubMed: 3083044]

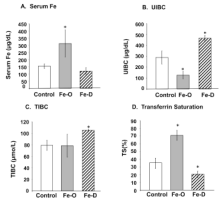

Fig. 1. Fe concentration in rats following FeO and FeD treatment

Rats were fed with FeO or FeD diet for 4 weeks. The Fe parameters were assayed by an Iron/TIBC testing kit. (A) Serum Fe levels. (B) Unsaturated Iron Binding Capacity (UIBC). (C) Total Iron Binding Capacity (TIBC). (D) Transferrin Saturation (TS). Data represent mean ± SEM, n=5-6. **=$p<0.01$; *=$p<0.05$.

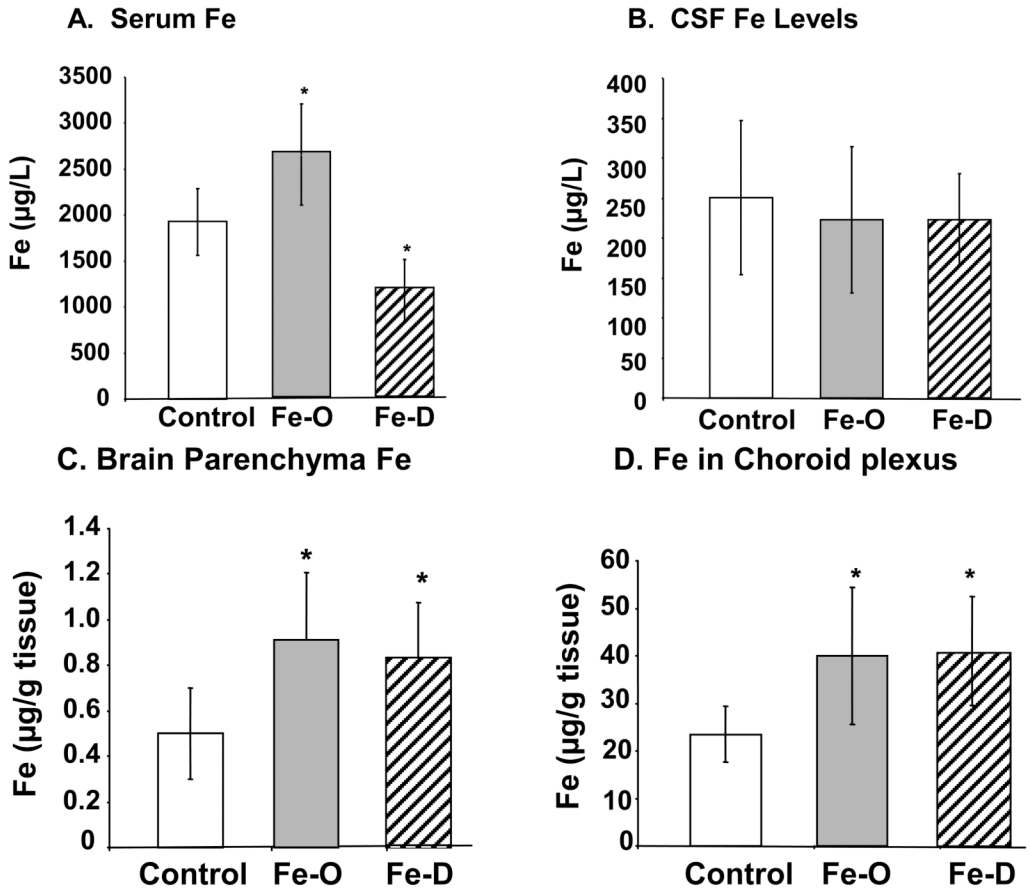

Fig. 2. Concentrations of Fe in serum, CSF, and brain parenchyma by ICP-MS analysis

Animal treatment is described in the legend to Fig. 1. (A) Fe levels in serum. (B) Fe levels in CSF. (C) Fe levels in brain parenchyma. Data represent mean ± S.D., n=5-6. **=$p<0.01$; *=$p<0.05$.

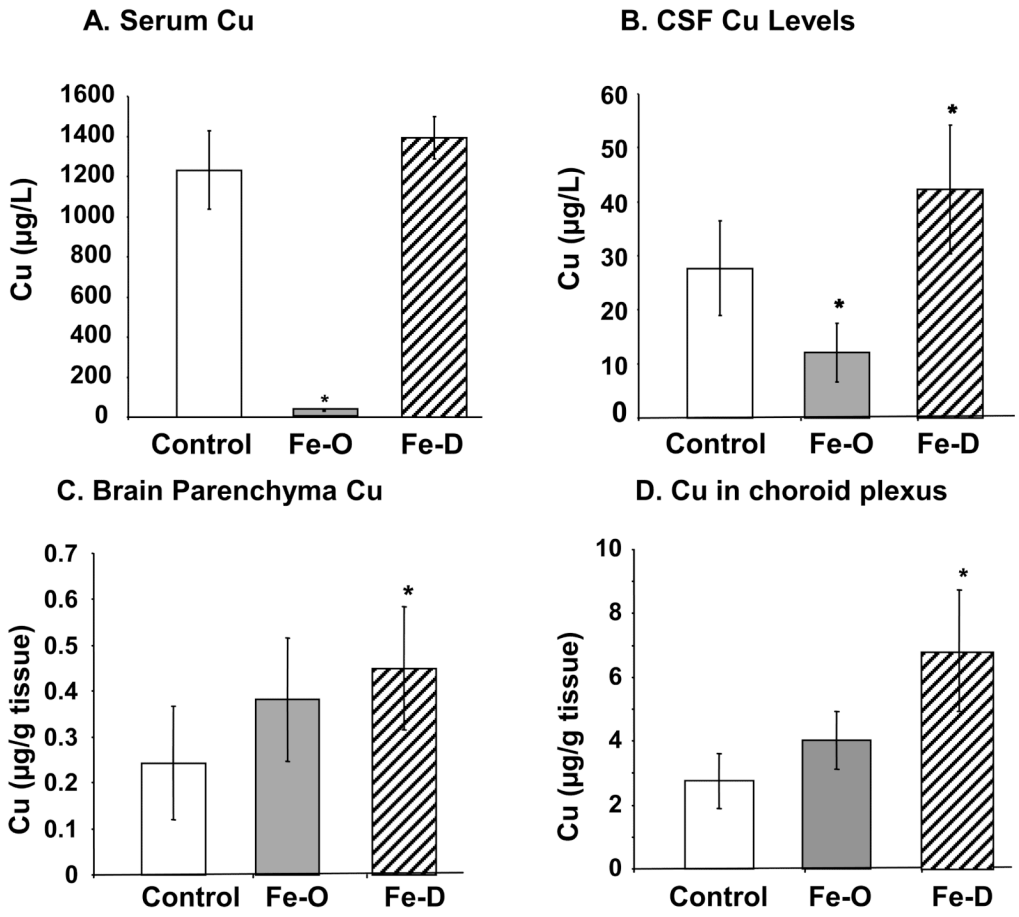

Fig. 3. Concentrations of Cu in serum, CSF, and brain parenchyma by ICP-MS analysis

Animal treatment is described in the legend to Fig. 1. (A) Cu levels in serum. (B) Cu levels in CSF. (C) Cu levels in brain parenchyma. Data represent mean ± S.D., n=5-6. **=p<0.01; *=p<0.05.

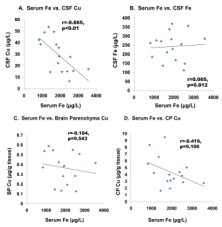

Fig. 4. Changes in CSF Cu, CSF Fe, choroid plexus Cu, and brain parenchyma Cu as a function of serum Fe levels

Animal treatment is described in the legend to Fig. 1. Data were analyzed by linear regression. (A) Cu in CSF ($r=-0.665$, $p<0.01$). (B) Fe in CSF ($r=-0.226$, $p=0.367$). (C) Cu in the CP ($r=-0.419$, $p=0.106$). (D) Cu in brain parenchyma ($r=-0.164$, $p=0.543$).

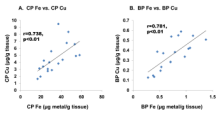

Fig. 5. Changes in tissue Cu levels as a function of tissue Fe levels

Animal treatment is described in the legend to Fig. 1. Data were analyzed by linear regression. (A) Cu-Fe in the choroid Plexus ($r=0.738$, $p<0.01$). (B) Cu-Fe in brain parenchyma ($r=0.781$, $p<0.01$) ($n=18$).

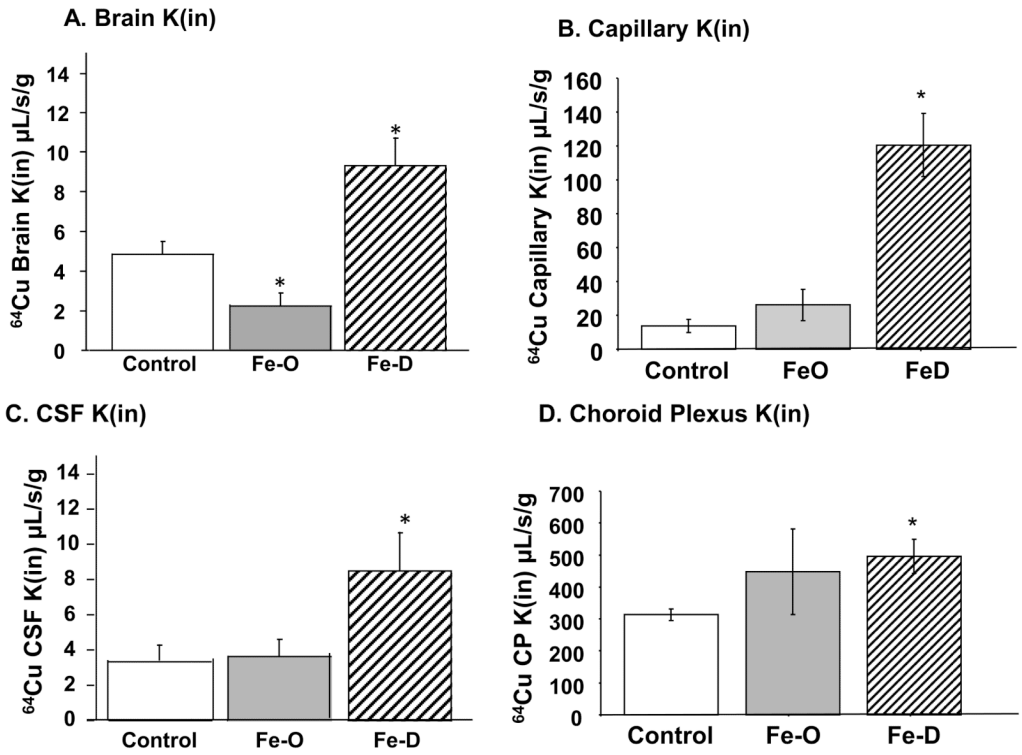

Fig. 6. Brain Cu transport by in situ brain perfusion technique

Animal treatment is described in the legend to Fig. 1. At the end of the treatment, brain was perfused with free ^{64}Cu for 5 min via the internal common carotid artery (A) Unidirectional transport rate constant (K_{in}) of Cu in brain parenchyma. (B) K_{in} of Cu in the brain capillaries. (C) K_{in} of Cu in CSF. (D) ^{64}Cu levels in the choroid plexus. Data represent mean ± SEM, n=3-5.

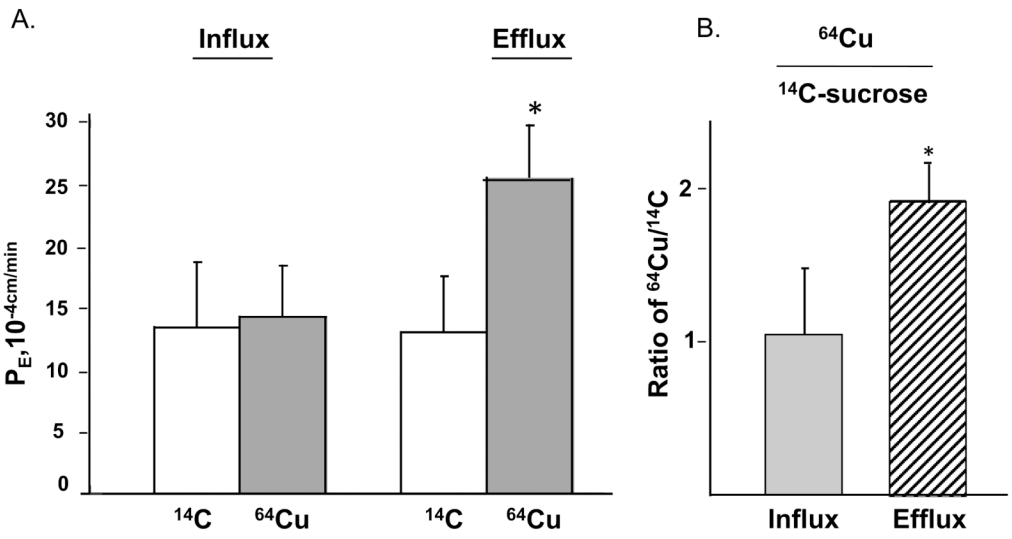

Fig. 7. Transport Cu by the BCB by the two chamber Transwell model

(A) Comparison of influx and efflux rates of free, unbound Cu in the two-chamber Transwell transport model. The influx or efflux rate of ^{64}Cu as determined by the PE value. ^{14}C-sucrose was used to determine non-specific paracellular leakage (B) Cu/C was the radioactivity of ^{54}Cu corrected by ^{14}C-sucrose. Data represents mean ±SD, n=4. *: $p<0.05$, influx vs. efflux.

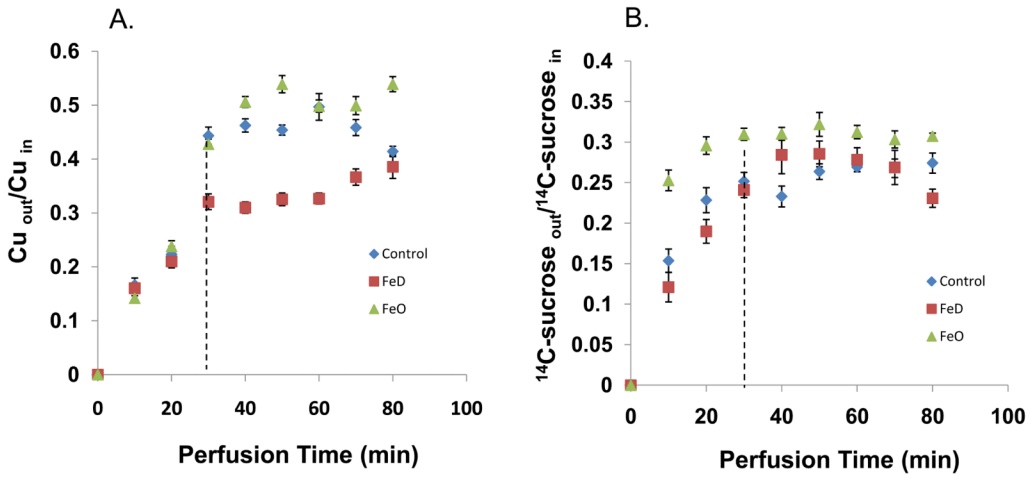

Fig. 8. Cu Clearance by the BCB

Effect of FeD and FeO on ^{64}Cu clearance and ^{14}C-sucrose clearance from the CSF by in situ ventriculo-cisternal brain perfusion. The artificial CSF (aCSF) containing either $^{64}CuCl_2$ or ^{14}C-sucrose was infused into the lateral ventricle of the rat brain and the CSF effluent was collected from the cistern magna. (A) ^{64}Cu clearance. Cu_{out}, Cu concentration in the collected cisternal effluent; Cu_{in}, Cu concentration in the perfusate into the lateral ventricle. (B) ^{14}C-sucrose clearance ^{14}C-sucrose$_{out}$, ^{14}C-sucrose concentration in the collected from the cisternal effluent; ^{14}C-sucrose$_{in}$, ^{14}C-sucrose concentration in the perfusate into the lateral ventricle. Data represent mean ± SEM, n=5-6.

Toxicol Appl Pharmacol. Author manuscript; available in PMC 2012 November 1.

Table 1

Effect of FeO or FeD on various metals in the Choroid Plexus, Brain Parenchyma, Serum, and CSF.

	Choroid Plexus (μg/g tissue)			**Brain Parenchyma (μg/g tissue)**		
Metals	**Control**	**Fe-Overload**	**Fe-Deficient**	**Control**	**Fe-Overload**	**Fe-Deficient**
Ca43	40.60 ± 17.20	81.70 ± 61.60	***210.0*** ± ***222.0*** ^{A}	40.40 ±13.30	***79.00*** ± ***15.10*** ^{A}	***67.90*** ± ***24.40*** ^{A}
Mn55	0.081 ± 0.040	0.168 ± 0.201	0.230 ± 0.121	0.024 ±0.010	0.038 ± 0.010	***0.042*** ± ***0.014***^{A}
Co59	0.027 ± 0.017	0.034 ± 0.008	***0.053*** ± ***0.015*** ^{A}	0.002 ± 0.003	0.004 ± 0.005	0.004 ± 0.005
Ni60	0.053 ± 0.025	0.092 ± 0.028	***0.146*** ± ***0.088*** ^{A}	0.003 ± 0.002	0.006 ± 0.002	***0.0070*** ± ***0.004*** ^{B}
Zn66	11.70 ± 3.400	17.80 ± 6.000	***26.60*** ± ***7.400*** ^{A}	1.020 ± 0.530	***1.980*** ± ***0.830*** ^{A}	1.760 ± 0.550
Se82	0.387 ± 0.110	0.605 ± 0.145	***0.865*** ± ***0.253*** ^{A}	0.017 ± 0.007	***0.034*** ± ***0.017*** ^{A}	0.030 ± 0.012
Rb85	0.480 ± 0.160	0.519 ± 0.140	***1.110*** ± ***0.320*** ^{A}	0.029 ±0.011	0.037 ± 0.017	0.039 ± 0.014
Sr88	0.005 ± 0.02370	0.051 ± 0.113	0.057 ± 0.050	0.024 ±0.006	***0.046*** ± ***0.012*** ^{A}	***0.036*** ± ***0.008*** ^{A}
	Serum (μg/L)			**CSF(μg/L)**		
Metals	**Control**	**Fe-Overload**	**Fe-Deficient**	**Control**	**Fe-Overload**	**Fe-Deficient**
Ca43	131000 ± 21200	152000 ± 20400	133000 ± 14400	37800 ± 18200	46800 ± 24700	50000 ± 14600
Mn55	0.663 ± 0.618	1.330 ± 1.030	0.524 ± 0.452	3.200 ± 0.820	1.650 ± 2.890	14.90 ± 17.90
Co59	0.529 ± 0.084	0.488 ± 0.053	***0.672*** ± ***0.106*** ^{A}	0.471 ± 0.146	0.401 ± 0.239	0.378 ± 0.047
Ni60	5.580 ± 4.220	4.490 ± 1.540	5.440 ± 1.700	3.470 ± 2.160	2.030 ± 1.280	1.970 ± 0.560
Zn66	1720 ± 390.0	1580 ± 390.0	1950 ± 458.0	162.0 ± 74.00	112.0 ± 48.00	142.0 ± 53.00
Se82	973.0 ± 283.0	855.0 ± 213.0	969.0 ± 255.0	25.30 ± 13.60	22.70 ± 9.390	***39.40*** ± ***7.090*** ^{A}
Rb85	124 ± 61	***72.80*** ± ***30.90*** ^{B}	82.40 ± 10.80	13.10 ± 5.600	9.910 ± 4.820	14.80 ± 3.20
Sr88	28.6 ± 5.6	***15.30*** ± ***2.400*** ^{B}	***21.20*** ± ***4.800*** ^{B}	6.630 ± 3.2900	***2.900*** ± ***1.840*** ^{B}	6.300 ± 2.410

Serum, CSF, capillary depleted brain parenchyma, and choroid plexus tissues were collected and analyzed for metal content via ICP-MS. Data represent mean ± SD (n=6).

^{A}significant increase;

^{B}significant decrease relative to control.